August 2007

# Fourier Decomposition Analysis af Anisotropic Inhomogeneous Dielectric Waveguide Structures

Ramin Pashaie
*University of Pennsylvania*, raminp@seas.upenn.edu

# Fourier Decomposition Analysis af Anisotropic Inhomogeneous Dielectric Waveguide Structures

**Abstract**
In this paper we extend the Fourier decomposition method to compute both propagation constants and the corresponding electromagnetic field distributions of guided waves in millimeter-wave and integrated optical structures. Our approach is based on field Fourier expansions of a pair of wave equations which have been derived to handle inhomogeneous mediums with diagonalized permittivity and permeability tensors. The tensors are represented either by a grid of homogeneous rectangles or by distribution functions defined over rectangular domains. Using the Fourier expansion, partial differential equations are converted to a matrix eigenvalue problem that correctly models this class of dielectric structures. Finally numerical results are presented for various channel waveguides and are compared with those of other literatures to validate our formulation.

**Keywords**
anisotropic, dielectric waveguide, fourier decomposition method, inhomogenous

# Fourier Decomposition Analysis of Anisotropic Inhomogeneous Dielectric Waveguide Structures

Ramin Pashaie, *Student Member, IEEE*

***Abstract*—In this paper, we extend the Fourier decomposition method to compute both propagation constants and the corresponding electromagnetic field distributions of guided waves in millimeter-wave and integrated optical structures. Our approach is based on field Fourier expansions of a pair of wave equations, which have been derived to handle inhomogeneous mediums with diagonalized permittivity and permeability tensors. The tensors are represented either by a grid of homogeneous rectangles or by distribution functions defined over rectangular domains. Using the Fourier expansion, partial differential equations are converted to a matrix eigenvalue problem that correctly models this class of dielectric structures. Finally, numerical results are presented for various channel waveguides and are compared with those of other literature to validate the formulation.**

***Index Terms*—Anisotropic, dielectric waveguide, Fourier decomposition method, inhomogenous.**

## I. Introduction

DIELECTRIC waveguides are widely used for the transmission of electromagnetic energy and in the structure of optical devices such as directional couplers and modulators at optical frequencies. As the design criteria for these devices become tighter, results of approximate methods often do not have the desired accuracy. Examples of approximate methods are the effective index method [1], [2], the semivectorial finite-difference method [3], [4], and the variational methods [5]. Rigorous techniques include the vector finite-element method (FEM) [6], [7], the domain integral-equation method [8]–[11], and the method of lines [12], [13]. The FEM is an exact and general technique that can be utilized in the analysis of inhomogeneous anisotropic dielectric waveguides. Despite flexibilities of such a numerical method, the incorporation of unbounded regions outside the waveguide and the occurrence of spurious solutions (as a result of inexplicit satisfaction of the divergence equation) are two major problems one has to face using this method. An important advantage of the domain integral-equation method is that it avoids spurious solutions; nevertheless, this method is time consuming. The method of lines is a rigorous seminumerical technique. It is well known for its accuracy, speed of computation, and minimal memory requirements; however, it is relatively complicated.

Manuscript received February 24, 2007; revised April 15, 2007.

The author is with the Electrical and System Engineering Department, University of Pennsylvania, Philadelphia, PA 19104 USA (e-mail: raminp@seas.upenn.edu).

Color versions of one or more of the figures in this paper are available online at http://ieeexplore.ieee.org.

Digital Object Identifier 10.1109/TMTT.2007.902616

In 1989, Henry and Verbeek proposed an interesting method for modal analysis of arbitrary shaped inhomogeneous dielectric waveguides with small changes in the refractive index function (weakly guiding) and negligible induced birefringence for modes that are far from their cutoff [14]. This analysis, which was further investigated by Marcuse [15], allows evaluation of propagation constants and field distributions within any desired precision. The method is based on expansion of the unknown field in a complete set of orthogonal functions within limited boundaries. which converts a linear partial differential equation into a matrix eigenvalue problem. By solving the eigenvalue problem, all the guided modes of the waveguide are clarified. Nevertheless, only those guided modes for which the field goes to zero before the boundary is reached are computed accurately.

More recently, Hewlett and Ladoucer improved this method by introducing a preliminary mapping of the infinite transverse plane onto a unit square by applying a suitable analytic transformation function [16]. This modification allows computation of even near-to-cutoff modes by using relatively few waves. The main drawback is that both computation time and memory requirements can become exceedingly large before adequate accuracy is obtained; however, this problem can be solved by using suitable optimization parameters. Henry and Verbeek's method can be used for modal analysis of inhomogeneous isotropic dielectric structures such as ion-exchange optical waveguides in the substrate of glass [17]. Nevertheless, extending the utility of this technique to applications that make use of anisotropic mediums (e.g., $LiNbO_3$) requires reformulation of the method.

In this paper, Henry and Verbeek's method is extended and applied to the vector form of the wave equation. With minimal increase in computation time and memory requirements, the method is improved for modal analysis of anisotropic inhomogeneous dielectric structures. Recently, independent of this study, other researchers have studied full vector analysis of inhomogeneous dielectric waveguides [18]–[20]. However, to the author's knowledge, the formulation in this paper covers the most general case, including anisotropic mediums.

Basic equations are derived in Section II followed by the description of the eigenvalue problem. In Section III, numerical results are presented and discussed. Finally, concluding remarks are made in Section IV.

## II. Formulation

Here, wave and field equations that must be solved are derived directly from Maxwell's equations. The Fourier expansion formulation is then applied to the developed equations so that an appropriate eigenvalue problem is obtained.

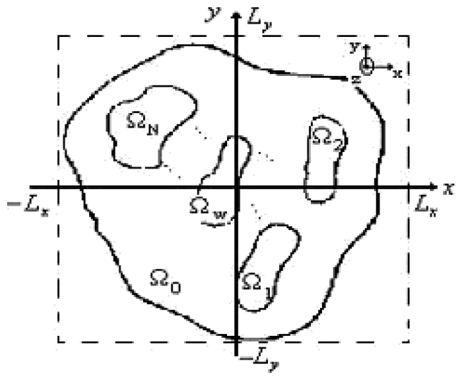


Fig. 1. Dielectric waveguiding structure with arbitrary shaped anisotropic inhomogeneous dielectric subregions $\Omega^1\Omega^2, \Omega^3, \ldots, \Omega^N$ and $\Omega^w$ embedded in $\Omega^0$ dielectric media.

### A. Basic Equations

Consider the case where an anisotropic inhomogeneous waveguiding region with arbitrary shape $\Omega^w$ is embedded within the substrate $\Omega^0$, and this embedding consists of $N$ other dielectric subregions $\Omega^1, \Omega^2, \Omega^3, \ldots, \Omega^N$. The cross section of such a dielectric structure is illustrated in Fig. 1. The position is specified using a right-handed Cartesian reference frame. The $z$-axis is chosen such that the material properties of the waveguide configuration is invariant in the $z$-direction. Each sub-domain is assumed to be anisotropic and inhomogeneous, with diagonal permittivity and permeability tensors as follows:

$$\begin{bmatrix} \epsilon_x(x,y) & 0 & 0 \\ 0 & \epsilon_y(x,y) & 0 \\ 0 & 0 & \epsilon_z(x,y) \end{bmatrix} \tag{1}$$

$$\begin{bmatrix} \mu_x(x,y) & 0 & 0 \\ 0 & \mu_y(x,y) & 0 \\ 0 & 0 & \mu_z(x,y) \end{bmatrix}. \tag{2}$$

Both dielectric and ohmic losses are included since $\epsilon_i$ and $\mu_i$ are taken to be complex quantities defined as $\mu_i = \mu_i' - j\mu_i''$ and $\epsilon_i = \epsilon_i' - j(\epsilon_i'' + \sigma_i/\omega)$, where $\sigma_i$ are components of the conductivity tensor. In a source-free anisotropic inhomogeneous medium, Maxwell's equations are written as follows:

$$\nabla \times \overline{E} = -j\omega\mu_0\overline{\mu} \cdot \overline{H} \tag{3}$$

$$\nabla \times \overline{H} = -j\omega\epsilon_0\overline{\epsilon} \cdot \overline{E} \tag{4}$$

$$\nabla \cdot (\overline{\mu} \cdot \overline{H}) = 0 \tag{5}$$

$$\nabla \cdot (\overline{\epsilon} \cdot \overline{E}) = 0. \tag{6}$$

Maxwell's curl equations (3) and (4) are coupled first-order differential equations. They become uncoupled by applying the following sequence of mathematical operations, $\nabla \times \overline{\mu}^{-1} \cdot$ (4) into (3) and $\nabla \times \overline{\epsilon}^{-1} \cdot$ (3) into (4). Second-order vector wave equations are then obtained for electric and magnetic fields

$$\nabla \times \overline{\mu}^{-1} \cdot \nabla \times \overline{E} - k_0^2 \overline{\epsilon} \cdot \overline{E} = 0 \tag{7}$$

$$\nabla \times \overline{\epsilon}^{-1} \cdot \nabla \times \overline{H} - k_0^2 \overline{\mu} \cdot \overline{H} = 0 \tag{8}$$

where the wavenumber $k_0$ is defined as $k_0^2 = \omega^2\mu_0\epsilon_0$. From the Gauss equations (5) and (6), we find that

$$\frac{\partial E_z}{\partial z} = \frac{-1}{\epsilon_z}\left[\frac{\partial}{\partial x}(\epsilon_x E_x) + \frac{\partial}{\partial y}(\epsilon_y E_y)\right] \tag{9}$$

$$\frac{\partial H_z}{\partial z} = \frac{-1}{\mu_z}\left[\frac{\partial}{\partial x}(\epsilon_x H_x) + \frac{\partial}{\partial y}(\epsilon_y H_y)\right]. \tag{10}$$

The two vector wave equations (7) and (8) can be further expanded into six scalar wave equations. In an inhomogeneous anisotropic medium, each scalar wave equation is coupled with at least one other, and solving these equations is prohibitively difficult. Nevertheless, uncoupled scalar wave equations can be developed by considering only the $\mathrm{TE}^x (E_x^{\mathrm{TE}} = 0)$ and $\mathrm{TM}^x (H_x^{\mathrm{TM}} = 0)$ modes and using (9) and (10) accordingly. The superposition of the $\mathrm{TE}^x$ and the $\mathrm{TM}^x$ modes will then completely characterize propagating modes (including hybrid modes) in the structure

$$\frac{\partial}{\partial y}\left[\frac{1}{\epsilon_z}\frac{\partial}{\partial y}\left(\epsilon_y E_y^{\mathrm{TE}}\right)\right] + \mu_x \frac{\partial}{\partial_x}\left[\frac{1}{\mu_z}\frac{\partial E_y^{\mathrm{TE}}}{\partial x}\right] + \left(k_0^2\epsilon_y\mu_x - \beta^2\right) E_y^{\mathrm{TE}} = 0 \tag{11}$$

$$\frac{\partial}{\partial y}\left[\frac{1}{\mu_z}\frac{\partial}{\partial y}\left(\mu_y H_y^{\mathrm{TM}}\right)\right] + \epsilon_x \frac{\partial}{\partial_x}\left[\frac{1}{\epsilon_z}\frac{\partial H_y^{\mathrm{TM}}}{\partial x}\right] + \left(k_0^2\epsilon_x\mu_y - \beta^2\right) H_y^{\mathrm{TM}} = 0. \tag{12}$$

Due to the continuity of $E_z$ and $H_z$ in all the regions and boundaries, in (11) and (12), one can change the order of differentiation in terms $\partial^2 E_z/\partial z\partial y$ and $\partial^2 H_z/\partial z\partial y$ to $\partial^2 E_z/\partial y\partial z$ and $\partial^2 H_z/\partial y\partial z$, respectively. Consequently, the $x$- and $z$-oriented electric and magnetic components of a propagating mode in this dielectric structure are related to the $\mathrm{TE}^x$- and $\mathrm{TM}^x$-mode components via the following set of equations:

$$E_x = \frac{1}{\beta}\left(\omega\mu_0\mu_y H_y^{\mathrm{TM}} + \frac{1}{\omega\epsilon_0\epsilon_z}\frac{\partial^2 H_y^{\mathrm{TM}}}{\partial x^2}\right) \tag{13}$$

$$H_x = \frac{1}{\beta}\left(\omega\epsilon_0\epsilon_y E_y^{\mathrm{TE}} + \frac{1}{\omega\mu_0\mu_z}\frac{\partial^2 E_y^{\mathrm{TE}}}{\partial x^2}\right) \tag{14}$$

$$E_z = j\left(\frac{1}{\epsilon_z\beta}\epsilon_y\frac{\partial E_y^{\mathrm{TE}}}{\partial y} - \frac{1}{\omega\epsilon_0\epsilon_z}\frac{\partial H_y^{\mathrm{TM}}}{\partial x}\right) \tag{15}$$

$$H_z = j\left(\frac{1}{\mu_z\beta}\mu_y\frac{\partial H_y^{\mathrm{TM}}}{\partial y} + \frac{1}{\omega\epsilon_0\epsilon_z}\frac{\partial E_y^{\mathrm{TE}}}{\partial x}\right) \tag{16}$$

$$E_y = E_y^{\mathrm{TE}} + \frac{1}{\beta\omega\epsilon_0\epsilon_z}\frac{\partial^2 H_y^{\mathrm{TM}}}{\partial y\partial x} \tag{17}$$

$$H_y = H_y^{\mathrm{TM}} - \frac{1}{\beta\omega\mu_0\mu_z}\frac{\partial^2 E_y^{\mathrm{TE}}}{\partial y\partial x}. \tag{18}$$

Finding an analytical solution for (11) and (12) is complicated and numerical (or seminumerical) methods are often preferred. In the Fourier decomposition method, all dielectric sub-domains $\Omega^1, \Omega^2, \Omega^3, \ldots, \Omega^N$ and $\Omega^w$ are enclosed in a virtual box whose dimensions are $2L_x$ and $2L_y$ along $x$- and $y$-axes, respectively. $L_x$ and $L_y$ are large enough to ensure that the electromagnetic fields of the guided modes are zero on these artificial boundaries.

The electric field of the $\mathrm{TE}^x$ mode and the magnetic field of the $\mathrm{TM}^x$ mode are then expanded in terms of a complete set of orthogonal basis functions $\phi = \{\phi_i\}_{i=1}^{\infty}$

$$E_y^{\mathrm{TE}} = \sum_{i=1}^{\infty} a_i \phi_i(x,y) \approx \sum_{i=1}^{N} a_i \phi_i(x,y) \tag{19}$$

$$H_y^{\mathrm{TM}} = \sum_{i=1}^{\infty} b_i \phi_i(x,y) \approx \sum_{i=1}^{N} b_i \phi_i(x,y). \tag{20}$$

In practice, infinite summations are approximated by considering finite terms in the expansions. The main restriction of the Fourier method appears as the modal cutoff is approached. Close to cutoff, more terms need to be included in the field expansion, and the bounding box should be chosen much larger to make the implicit assumption of zero field on the boundary more reasonable. An explicit solution to this difficulty is proposed in [16] in which the whole $x$–$y$-plane is mapped onto a unit square in the $u$–$v$-plane via analytical transformation functions such as

$$x = \alpha_x \tan\left[\pi\left(u - \frac{1}{2}\right)\right] \tag{21}$$

$$y = \alpha_y \tan\left[\pi\left(v - \frac{1}{2}\right)\right] \tag{22}$$

where $\alpha_x$ and $\alpha_y$ are arbitrary scaling parameters. With this mapping, boundary conditions for all bounded modes are satisfied automatically. One can develop the $\mathrm{TE}^x$ and $\mathrm{TM}^x$ characteristic wave equations in transformed coordinates by applying the mapping equations (21) and (22) to (11) and (12) as follows:

$$\begin{aligned}
&\left\{\frac{\epsilon_y}{\epsilon_z}\left[\left(\frac{dv}{dy}\right)^2\frac{\partial^2}{\partial v^2} + \frac{d^2v}{dy^2}\frac{\partial}{\partial v}\right]\right.\\
&\quad + \frac{\mu_x}{\mu_y}\left[\left(\frac{du}{dx}\right)^2\frac{\partial^2}{\partial u^2} + \frac{d^2u}{dx^2}\frac{\partial}{\partial u}\right]\\
&\quad + \left[\frac{1}{\epsilon_z}\frac{\partial \epsilon_y}{\partial v} + \frac{\partial}{\partial v}\left(\frac{\epsilon_y}{\epsilon_z}\right)\right]\left[\frac{dv}{dy}\right]\frac{\partial}{\partial v} + \mu_x\frac{\partial}{\partial u}\left[\frac{1}{\mu_z}\right]\frac{du}{dx}\frac{\partial}{\partial u}\\
&\quad \left.+ \left[\frac{\partial}{\partial v}\left(\frac{1}{\epsilon_z}\frac{\partial \epsilon_y}{\partial v}\right) + k_0^2\mu_x\epsilon_y - \beta^2\right]\right\} E_y^{\mathrm{TE}} = 0
\end{aligned} \tag{23}$$

$$\begin{aligned}
&\left\{\frac{\mu_y}{\mu_z}\left[\left(\frac{dv}{dy}\right)^2\frac{\partial^2}{\partial v^2} + \frac{d^2v}{dy^2}\frac{\partial}{\partial v}\right]\right.\\
&\quad + \frac{\epsilon_x}{\epsilon_y}\left[\left(\frac{du}{dx}\right)^2\frac{\partial^2}{\partial u^2} + \frac{d^2u}{dx^2}\frac{\partial}{\partial u}\right]\\
&\quad + \left[\frac{1}{\mu_z}\frac{\partial \mu_y}{\partial v} + \frac{\partial}{\partial v}\left(\frac{\mu_y}{\mu_z}\right)\right]\left[\frac{dv}{dy}\right]\frac{\partial}{\partial v} + \epsilon_x\frac{\partial}{\partial u}\left[\frac{1}{\epsilon_z}\right]\frac{du}{dx}\frac{\partial}{\partial u}\\
&\quad \left.+ \left[\frac{\partial}{\partial v}\left(\frac{1}{\mu_z}\frac{\partial \mu_y}{\partial v}\right) + k_0^2\mu_y\epsilon_x - \beta^2\right]\right\} H_y^{\mathrm{TM}} = 0.
\end{aligned} \tag{24}$$

Solving these two Sturm–Liouville wave equations is the subject of Section II-B.

### *B. Eigenvalue Problem*

Consider the following orthogonal functions $\phi_{m_i,n_i}^{(i)}$:

$$\phi_{m_i,n_i}^{(1)} = 2\sin(m_i\pi u)\sin(n_i\pi v) \tag{25}$$

$$\phi_{m_i,n_i}^{(2)} = 2\cos\left[(m_i-1)\pi u\right]\sin(n_i\pi v) \tag{26}$$

$$\phi_{m_i,n_i}^{(3)} = 2\sin(m_i\pi u)\cos\left[(n_i-1)\pi v\right] \tag{27}$$

$$\phi_{m_i,n_i}^{(4)} = 2\sin\left[(m_i-1)\pi u\right]\cos\left[(n_i-1)\pi v\right]. \tag{28}$$

In these equations, $m_i$ and $n_i$ are nonnegative integers. Next, we expand the electric field $E_y^{\mathrm{TE}}$ and the magnetic field $H_y^{\mathrm{TM}}$ using $\phi_i^{(3)}(u,v)$ and the $\phi_i^{(2)}(u,v)$ functions, respectively,

$$\begin{aligned}
E_y^{\mathrm{TE}} &= e^{-j\beta z}\sum_{i=1}^{N_mN_n} a_i\phi_i^{(3)}(u,v)\\
&= e^{-j\beta z}\sum_{m_i=1}^{N_m}\sum_{n_i=0}^{N_n} a_{m_i,n_i}\phi_{m_i,n_i}^{(3)}(u,v)
\end{aligned} \tag{29}$$

$$\begin{aligned}
H_y^{\mathrm{TM}} &= e^{-j\beta z}\sum_{i=1}^{N_mN_n} b_i\phi_i^{(2)}(u,v)\\
&= e^{-j\beta z}\sum_{m_i=0}^{N_m}\sum_{n_i=1}^{N_n} b_{m_i,n_i}\phi_{m_i,n_i}^{(2)}(u,v)
\end{aligned} \tag{30}$$

where the indices $m_i$ and $n_i$ are

$$m_i = (i-1)\ \mathrm{div}\ (N_n) + 1 \tag{31}$$

$$n_i = (i-1)\bmod (N_n) + 1. \tag{32}$$

In the Fourier decomposition method, boundary conditions at the interfaces between the dielectrics are not applied directly. The field distribution functions are assumed to be piecewise smooth, continuous, and square integrable over the entire space. However, the jump discontinuity of the fields at the dielectric interfaces causes the appearances of the Gibbs phenomena. As a result, the solution of the vector wave equation is in good agreement with the exact solution, except on the dielectric interfaces. Nevertheless, the energy of this systematic error depresses with an increasing number of terms in the series expansion [15].

Substituting (29) and (30) into characteristic equations (23) and (24), multiplying by $\phi_{m_j,n_j}^{(3)}$ and $\phi_{m_j,n_j}^{(2)}$, respectively, and integrating over the unit square, the matrix eigenvalue equations will be developed for both TE and TM modes. For the electric field,

$$\begin{aligned}
&\sum_{i=1}^{N_mN_n}(V^2A_{j,i} + B_{j,i} - W^2C_{j,i})a_i\\
&\qquad = 0
\end{aligned} \tag{33}$$

$$A_{j,i} = \int_0^1\int_0^1 g(u,v)\phi_i^{(3)}(u,v)\phi_j^{(3)}(u,v)dudv \tag{34}$$

$$B_{j,i} = \rho^2(I_1 + I_2 + I_3 + I_4 + I_5 + I_6 + I_7) \tag{35}$$

$$C_{j,i} = \delta_{m_i,m_j}\left(\delta_{n_i,1}\delta_{n_j,1} + \delta_{n_i,n_j}\right) \tag{36}$$

$$g(u,v) = \frac{\mu_x\epsilon_y - (\mu_x)_{\mathrm{Min}}(\epsilon_y)_{\mathrm{Min}}}{(\mu_x)_{\mathrm{Max}}(\epsilon_y)_{\mathrm{Max}} - (\mu_x)_{\mathrm{Min}}(\epsilon_y)_{\mathrm{Min}}} \tag{37}$$

$$V = k_0\rho\sqrt{(\mu_x)_{\mathrm{Max}}(\epsilon_y)_{\mathrm{Max}} - (\mu_x)_{\mathrm{Min}}(\epsilon_y)_{\mathrm{Min}}} \tag{38}$$

$$W = \rho\sqrt{\beta^2 - k_0^2(\mu_x)_{\mathrm{Min}}(\epsilon_y)_{\mathrm{Min}}} \tag{39}$$

while for the magnetic field,

$$\sum_{i=1}^{N_m N_n} \left(V'^2 A'_{j,i} + B'_{j,i} - W'^2 C'_{j,i}\right) b_i = 0 \tag{40}$$

$$A'_{j,i} = \int_0^1 \int_0^1 g'(u,v)\phi_i^{(3)}(u,v)\phi_j^{(3)}(u,v)dudv \tag{41}$$

$$B'_{j,i} = \rho^2 \left(I'_1 + I'_2 + I'_3 + I'_4 + I'_5 + I'_6 + I'_7\right) \tag{42}$$

$$C'_{j,i} = \delta_{m_i,m_j}\left(\delta_{n_i,1}\delta_{n_j,1} + \delta_{n_i,n_j}\right) \tag{43}$$

$$g'(u,v) = \frac{\mu_y \epsilon_x - (\mu_y)_{\min}(\epsilon_x)_{\min}}{(\mu_y)_{\max}(\epsilon_x)_{\max} - (\mu_y)_{\min}(\epsilon_x)_{\min}} \tag{44}$$

$$V' = k_0 \rho \sqrt{(\mu_y)_{\max}(\epsilon_x)_{\max} - (\mu_y)_{\min}(\epsilon_x)_{\min}} \tag{45}$$

$$W' = \rho \sqrt{\beta^2 - k_0^2 (\mu_y)_{\min}(\epsilon_x)_{\min}}. \tag{46}$$

In these equations, $\rho$ is a normalization parameter that represents dimension of the dielectric waveguide. The variables $V$ and $V'$ are the waveguide's degree of guidance and $W$ and $W'$ are the modal cladding parameters [16]. The expressions for the double integrals $I_{1-7}$ and $I'_{1-7}$ are found in Appendix I.

Equations (33)–(39) and (40)–(46) express the eigenvalue problems, which can be readily solved using standard numerical routines. The eigenvalues $W^2$ and $W'^2$ and the corresponding eigenvectors $\overline{a} = (a_1, a_2, a_3, \ldots, a_{N_m N_n})^T$ and $\overline{b} = (b_1, b_2, b_3, \ldots, b_{N_m N_n})^T$ of the system matrices $C_{j,i}^{-1} = (V^2 A_{j,i} + B_{j,i})$ and $C'^{-1}_{j,i} = (V'^2 A'_{j,i} + B'_{j,i})$ yield the unknown modal propagation constants and the associated Fourier expansion coefficients, respectively. The modal fields can then be readily reconstructed in the $u-v$ space via (19) and (20) and mapped back to the $x-y$ space with the transformation functions (21) and (22).

These system matrices are $N_m N_n \times N_m N_n$ in size. Consequently, they possess $N_m N_n$ eigenvalues, including both bounded and continuum modes of the waveguide. Eigenvalues between the minimum of $\kappa_0^2(\mu_x)_{\min}(\epsilon_y)_{\min}$ and the maximum of $\kappa_0^2(\mu_x)_{\max}(\epsilon_y)_{\max}$ in the $\mathrm{TE}^x$ mode, and eigenvalues between the minimum of $\kappa_0^2(\mu_y)_{\min}(\epsilon_x)_{\min}$ and the maximum of $\kappa_0^2(\mu_y)_{\max}(\epsilon_x)_{\max}$ in the $\mathrm{TM}^x$ mode, are related to the bounded modes. At modal cutoff, the propagation constant $\beta^2$ is equal to $\kappa_0^2(\mu_x)_{\min}(\epsilon_y)_{\min}$ for the $\mathrm{TE}^x$ mode, and $\kappa_0^2(\mu_y)_{\min}(\epsilon_x)_{\min}$ for the $\mathrm{TM}^x$ mode. Thus, at the cutoff, $W^2 = W'^2 = 0$ and (33) and (40) are simplified to the following forms:

$$\sum_{i=1}^{N_m N_n} (V^2 A_{j,i} + B_{j,i}) a_i = 0 \tag{47}$$

$$\sum_{i=1}^{N_m N_n} \left(V'^2 A'_{j,i} + B'_{j,i}\right) b_i = 0. \tag{48}$$

In particular, the eigenvalues $1/V_{co}^2$ and $1/V_{co}'^2$ and the eigenvectors $\overline{a} = (a_1, a_2, a_3, \ldots, a_{N_m N_n})^T$ and $\overline{b} = (b_1, b_2, b_3, \ldots, b_{N_m N_n})^T$ of the system matrices $-B_{j,i}^{-1} A_{j,i}$ and $-B'^{-1}_{j,i} A'_{j,i}$ yield the cutoff values of $V$ and $V'$ and the associated Fourier expansion coefficients, respectively. As before, it is then straightforward to reconstruct the modal fields at the cutoff using (19) and (20) and the transformation functions (21) and (22).

Double integrals $I_{1-7}$ and $I'_{1-7}$ are the kernels of the Fourier decomposition method. Speed and accuracy of results obtained are critically affected by the way these integrals are computed. Generally, it is more convenient to describe the cross section of dielectric waveguides (particularly the waveguides formed from etched layers or those fabricated by diffusion process) as a series of rectangular meshes where the electromagnetic permittivity and permeability tensors are approximately constant over each mesh. In this case, $I_{1-5}$ and $I'_{1-5}$ are zero and closed-form equations can be written for other integrals. An efficient procedure for this purpose is presented in Appendix II.

Rapid increase in the computation time, which is of order $(N_m N_n)^3$ for each eigenvalue problem, is the main disadvantage of this method. Nevertheless, accurate results are often developed before a great increase in the computation time occurs. Moreover, by adjusting scaling parameters $\alpha_x$ and $\alpha_y$ and the normalization coefficient $\rho$, accurate results can be obtained by using minimal terms in the field expansions. For a channel dielectric waveguide with dimensions $dx$ and $dy$, optimum values for $\alpha_x$ and $\alpha_y$ are $dx/2$ and $dy/2$ and the optimum value for normalization parameter $\rho$ is the geometrical average of $\alpha_x$ and $\alpha_y$ [16]. Quasi-optimum values of the mapping parameters can be chosen automatically by utilization of adaptive techniques [21].

Finally, it should be noticed that an appropriate selection of the orthogonal basis functions reduces the number of required terms in the expansions and considerably affects the precision of results and the computation time. Selection of the orthogonal functions depends on the geometry of the structure. As an example, for multilayer cylindrical dielectric structures, such as optical fibers, Fourier Bessel expansion would be the best choice.

## III. Numerical Results

To validate the performance of the method, we defined three dielectric waveguides and analyzed them at optical frequencies. The results are obtained by employing the formulation given above. In each case, we compared our results with other available literatures. We adopt the modal identification format found in [22].

### A. Anisotropic Dielectric Waveguide

As a first example, an optical channel waveguide with rectangular cross section, embedded in a uniform media, is analyzed. The relative permittivities of the waveguide are $\epsilon_x = \epsilon_z = 2.31$, $\epsilon_y = 2.19$, and $\epsilon_b = 2.05$ for the background. The scaling parameters are chosen to be $\alpha_x = b$ and $\alpha_y = b/2$ and the normalization parameter is $\rho = \sqrt{\alpha_x \alpha_y}$. In each direction, 15 terms are considered in the expansions.

Fig. 2 illustrates the dispersion curves for the first four guided modes of the waveguide. The results are compared with data obtained from the method of lines [12] and FEM [7]. As can be seen, close correspondence exists. The normalized field distribution of the $E_x^{11}$ mode for $\beta_0 b = 4.0$ is depicted in Fig. 3.

### B. $LiNbO_3$ Optical Waveguide

As a second example, an anisotropic $LiNbO_3$ channel waveguide has been analyzed. The rectangular waveguide is surrounded by a uniform substrate with slightly smaller permeability tensors and homogeneous superstrate (air) that covers the

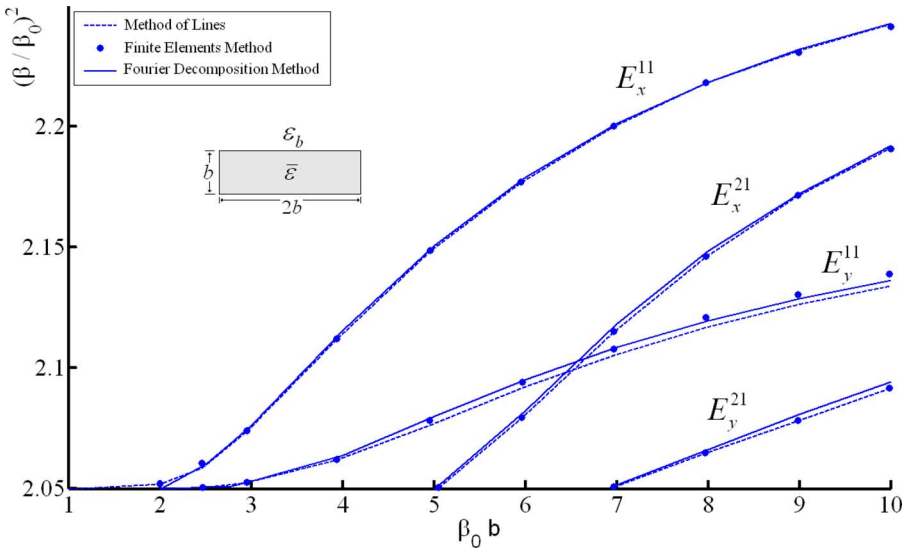


Fig. 2. Dispersion cures for the first four modes of the illustrated channel waveguide. Relative permeability tensor of the channel is $\epsilon_x = \epsilon_z = 2.31$, $\epsilon_y = 2.19$, and $\epsilon_b = 2.05$ for background. $\alpha_x = b$, $\alpha_y = b/2$, and $\rho = \sqrt{\alpha_x \alpha_y}$. Expansions with 15 terms in each direction are used.

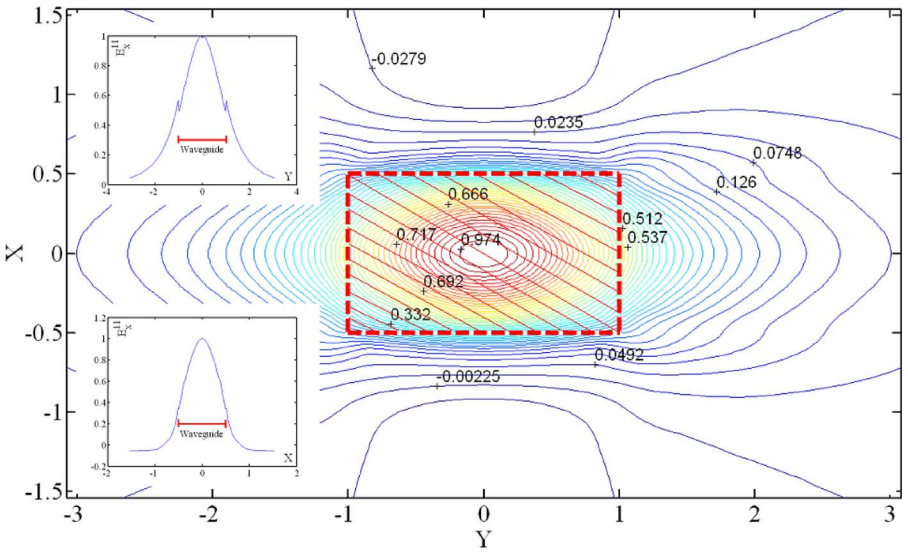


Fig. 3. Normalized field distribution of the $E_x^{11}$ mode in the anisotropic optical waveguide (the first numerical example) for $\beta_0 b = 4.0$.

structure. Relative permeability tensor in the channel is $\epsilon_x^c = 2.22^2$, $\epsilon_y^c = \epsilon_z^c = 2.3129^2$, and in the substrate, $\epsilon_y^s = \epsilon_z^s = 2.29^2$. In this case, physical dimensions of the channel is $2b \times b$, where $b = 1.0$ $\mu$m. The optimization parameters are chosen to be $\alpha_x = 2.5b$, $\alpha_y = b/2$, and the normalization parameter is $\rho = \sqrt{\alpha_x \alpha_y}$. Similar to the previous example, expansions with 15 terms in each direction are used. Fig. 4 illustrates the normalized dispersion curves of the guided modes $E_y^{11}$ and $E_y^{41}$ of the waveguide. As before, we compare the results with the method of lines [12] and FEM [6]. The cutoff wavelengths of these two modes can be computed with the direct procedure studied before. For instance, the normalized propagation constant of the $E_y^{41}$ mode is $(\beta_0 b)_{C0} = 1.03054$, which is computed using $25 \times 25$ expansion.

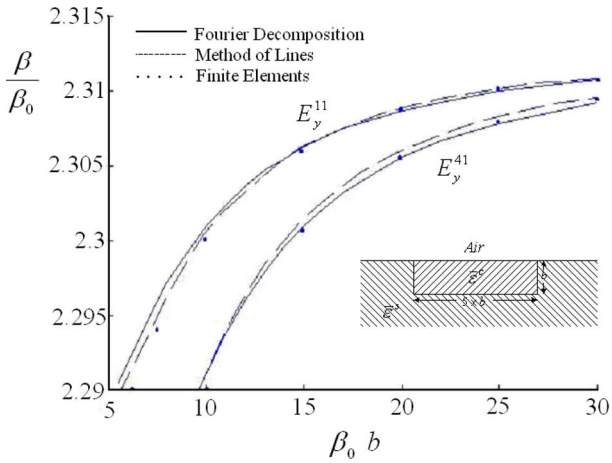


Fig. 4. Dispersion cures for the $E_y^{11}$ and $E_y^{41}$ modes of the illustrated waveguide. Relative permeability tensor in the channel is $\epsilon_x^c = 2.22^2$, $\epsilon_y^c = \epsilon_z^c = 2.3129^2$, and in the substrate, $\epsilon_y^s = \epsilon_z^s = 2.29^2$, for background. In this case, $b = 1.0$ $\mu$m, $\alpha_x = 2.5b$, $\alpha_y = b/2$, and $\rho = \sqrt{\alpha_x \alpha_y}$. Field expansions with 15 terms in each direction.

### C. Channel Waveguide With Permittivity and Permeability Tensors

As a final example, a channel waveguide with permittivity and permeability tensors is analyzed three times for three dif-

| | Case1 | Case2 | Case3 |
|---|---|---|---|
| $\overline{\varepsilon}_r$ | $\varepsilon_{xx,r}=2.6$ | $\varepsilon_{xx,r}=2.4$ | $\varepsilon_{xx,r}=2.8$ |
| | $\varepsilon_{yy,r}=2.6$ | $\varepsilon_{yy,r}=2.8$ | $\varepsilon_{yy,r}=2.4$ |
| | $\varepsilon_{zz,r}=2.6$ | $\varepsilon_{zz,r}=2.6$ | $\varepsilon_{zz,r}=2.6$ |
| $\overline{\mu}_r$ | $\mu_{xx,r}=1.10$ | $\mu_{xx,r}=1.15$ | $\mu_{xx,r}=1.05$ |
| | $\mu_{yy,r}=1.10$ | $\mu_{yy,r}=1.05$ | $\mu_{yy,r}=1.15$ |
| | $\mu_{zz,r}=1.10$ | $\mu_{zz,r}=1.10$ | $\mu_{zz,r}=1.10$ |

Fig. 5. Permittivity and permeability tensors of the channel waveguide in the last example.

ferent permittivity and permeability tensors that are listed in the table in Fig. 5. Fig. 6 illustrates the dispersion curves of the first two guided modes $E_y^{11}$ and $E_x^{11}$ in each of the three cases and compares the results with results obtained via the method of lines [12]. In spite of small differences in dispersion curves at lower frequencies, the dispersion curves we obtained agree quite well with other literature.

## IV. Summary

In this paper, the Fourier decomposition method has been extended to determine both propagation constants and modal field distributions of the guided modes in anisotropic inhomogeneous dielectric structures with arbitrary cross sections. The method has been successfully applied in numerical computation of the propagation constants of channel waveguides with second rank electromagnetic permittivity and permeability tensors.

## Appendix I

$I_{1-7}$ are the following integrals:

$$I_1=-(n_i-1)^2\pi^2\int_0^1\int_0^1\frac{\epsilon_y}{\epsilon_z}\left[\frac{dv}{dy}\right]^2\phi_i^{(3)}(u,v)\phi_j^{(3)}(u,v)dudv$$

$$I_2=-(n_i-1)\pi\int_0^1\int_0^1\frac{\epsilon_y}{\epsilon_z}\left[\frac{d^2v}{dy^2}\right]\phi_i^{(1)}(u,v)\phi_j^{(3)}(u,v)dudv$$

$$I_3=-m_i^2\pi^2\int_0^1\int_0^1\frac{\mu_y}{\mu_z}\left[\frac{du}{dx}\right]^2\phi_i^{(3)}(u,v)\phi_j^{(3)}(u,v)dudv$$

$$I_4=m_i\pi\int_0^1\int_0^1\frac{\mu_y}{\mu_z}\left[\frac{d^2u}{dx^2}\right]\phi_i^{(4)}(u,v)\phi_j^{(3)}(u,v)dudv$$

$$I_5=-(n_i-1)\pi\int_0^1\int_0^1\left[\frac{1}{\epsilon_z}\frac{\partial\epsilon_y}{\partial y}+\frac{\partial}{\partial y}\left(\frac{\epsilon_y}{\epsilon_z}\right)\right]\left[\frac{dv}{dy}\right]\times\phi_i^{(1)}(u,v)\phi_j^{(3)}(u,v)dudv$$

$$I_6=m_i\pi\int_0^1\int_0^1\left[\mu_x\frac{\partial}{\partial x}\left(\frac{1}{\mu_z}\right)\right]\left[\frac{du}{dx}\right]\times\phi_i^{(4)}(u,v)\phi_j^{(3)}(u,v)dudv$$

$$I_7=\int_0^1\int_0^1\left[\frac{\partial}{\partial y}\left(\frac{1}{\epsilon_z}\frac{\partial\epsilon_y}{\partial y}\right)\right]\phi_i^{(3)}(u,v)\phi_j^{(3)}(u,v)dudv \quad (49)$$

and $I'_{1-7}$ are as follows:

$$I'_1=-n_i^2\pi^2\int_0^1\int_0^1\frac{\mu_y}{\mu_z}\left[\frac{dv}{dy}\right]^2\phi_i^{(2)}(u,v)\phi_j^{(2)}(u,v)dudv$$

$$I'_2=n_i\pi\int_0^1\int_0^1\frac{\mu_y}{\mu_z}\left[\frac{d^2v}{dy^2}\right]\phi_i^{(4)}(u,v)\phi_j^{(2)}(u,v)dudv$$

$$I'_3=-(m_i-1)^2\pi^2\int_0^1\int_0^1\frac{\epsilon_x}{\epsilon_z}\left[\frac{du}{dx}\right]^2\times\phi_i^{(2)}(u,v)\phi_j^{(2)}(u,v)dudv$$

$$I'_4=-(m_i-1)\pi\int_0^1\int_0^1\frac{\epsilon_x}{\epsilon_z}\left[\frac{d^2u}{dx^2}\right]\phi_i^{(1)}(u,v)\phi_j^{(2)}(u,v)dudv$$

$$I'_5=n_i\pi\int_0^1\int_0^1\left[\frac{1}{\mu_z}\frac{\partial\mu_y}{\partial y}+\frac{\partial}{\partial y}\left(\frac{\mu_y}{\mu_z}\right)\right]\left[\frac{dv}{dy}\right]\times\phi_i^{(4)}(u,v)\phi_j^{(2)}(u,v)dudv,$$

$$I'_6=(m_i-1)\pi\int_0^1\int_0^1\left[\epsilon_x\frac{\partial}{\partial x}\left(\frac{1}{\epsilon_z}\right)\right]\left[\frac{du}{dx}\right]\times\phi_i^{(1)}(u,v)\phi_j^{(2)}(u,v)dudv$$

$$I'_7=\int_0^1\int_0^1\left[\frac{\partial}{\partial y}\left(\frac{1}{\mu_z}\frac{\partial\mu_y}{\partial y}\right)\right]\phi_i^{(2)}(u,v)\phi_j^{(2)}(u,v)dudv. \quad (50)$$

## Appendix II

Here, the closed-form equations are presented as follows for computation of $I_1-I_4$ and $I'_1-I'_4$ when the permittivity and permeability tensors are constant on a rectangular mesh (our standard rectangular mesh is depicted in Fig. 7):

$$I_1=\frac{-4n_i^2\left(\frac{\epsilon y}{\epsilon z}\right)}{\alpha_y^2}P_a^b(m_i,m_j)\times\big(0.1875S_c^d(n_i+n_j)+0.1875S_c^d(n_i-n_j)-0.25Q_c^d(n_i+n_j,2)-0.25Q_c^d(n_i-n_j,2)+0.0625Q_c^d(n_i+n_j,4)+0.0625Q_c^d(n_i-n_j,4)\big)$$

$$I_2=\frac{-8n_i\left(\frac{\epsilon y}{\epsilon z}\right)}{\alpha_y^2}P_a^b(m_i,m_j)\times\big(0.125P_a^b(n_i+n_j,2)+0.125P_c^d(n_i-n_j,2)-0.0625Q_c^d(n_i+n_j,4)-0.0625Q_c^d(n_i-n_j,4)\big)$$

$$I_3=\frac{-4m_i^2\left(\frac{\mu y}{\mu z}\right)}{\alpha_x^2}Q_c^d(n_i,n_j)\times\big(-0.1875S_a^b(m_i+m_j)-0.1875S_a^b(m_i-m_j)+0.25Q_a^b(m_i+m_j,2)-0.25Q_a^b(m_i-m_j,2)-0.0625Q_a^b(m_i+m_j,4)-0.0625Q_a^b(m_i-m_j,4)\big)$$

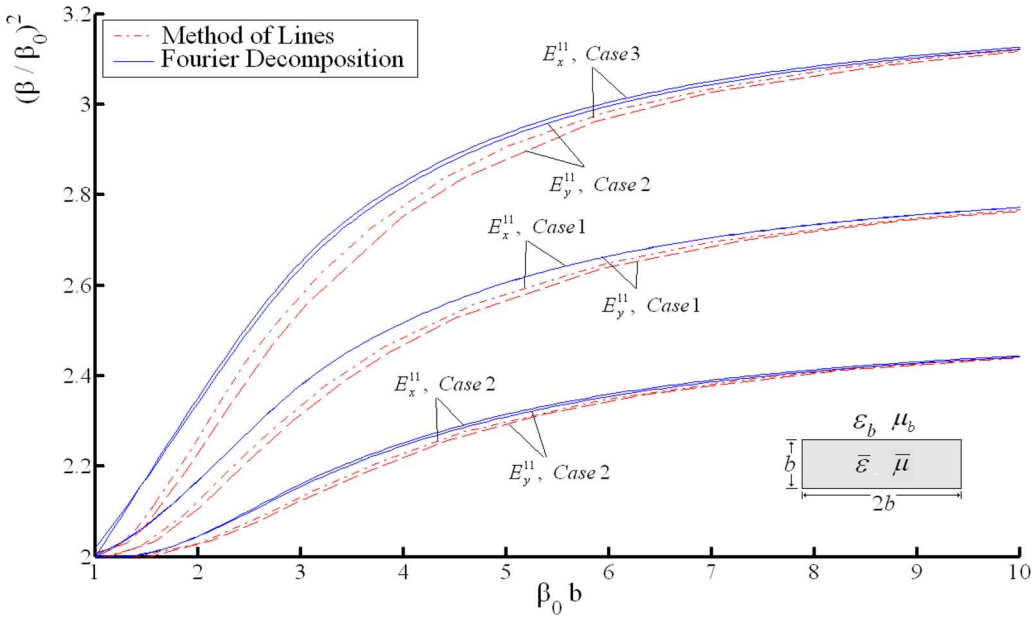


Fig. 6. Dispersion curves of illustrated channel waveguide with permittivity and permeability tensors. $\alpha_x = 2.5b$, $\alpha_y = b/2$, and $\rho = \sqrt{\alpha_x \alpha_y}$. Field expansions include 15 terms in each direction.

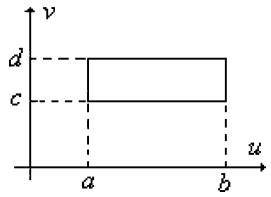


Fig. 7. Standard rectangular mesh.

$$I_4 = \frac{8m_i\left(\frac{\mu y}{\mu z}\right)}{\alpha_y^2} Q_c^d(n_i,n_j) \times \left(0.125P_a^b(m_i+m_j,2)+0.125P_a^b(m_i-m_j,2) - 0.0625P_a^b(m_i+m_j,4)-0.0625P_a^b(m_i-m_j,4)\right)$$

$$I_1' = \frac{-4n_i^2\left(\frac{\mu y}{\mu z}\right)}{\alpha_y^2} Q_a^b(m_i,m_j) \times \left(-0.1875S_a^b(n_i+n_j)-0.1875S_a^b(n_i-n_j) + 0.25Q_c^d(n_i+n_j,2)-0.25Q_c^d(n_i-n_j,2) -0.0625Q_c^d(n_i+n_j,4)-0.0625Q_c^d(n_i-n_j,4)\right)$$

$$I_2' = \frac{8n_i\left(\frac{\mu y}{\mu z}\right)}{\alpha_y^2} Q_a^b(m_i,m_j) \times \left(0.125P_c^d(n_i+n_j,2)+0.125P_c^d(n_i-n_j,2) - 0.0625Q_c^d(n_i+n_j,4)-0.0625Q_c^d(n_i-n_j,4)\right)$$

$$I_3' = \frac{-4m_i^2\left(\frac{\epsilon y}{\epsilon z}\right)}{\alpha_x^2} P_c^d(n_i,n_j) \times \left(0.1875S_a^b(m_i+m_j)+0.1875S_a^b(m_i-m_j) - 0.25Q_a^b(m_i+m_j,2) - 0.25Q_a^b(m_i-m_j,2) +0.0625Q_a^b(m_i+m_j,4)+0.0625Q_a^b(m_i-m_j,4)\right).$$

$$I_4' = \frac{8m_i\left(\frac{\epsilon y}{\epsilon z}\right)}{\alpha_y^2} P_c^d(n_i,n_j) \times \left(0.125P_a^b(m_i+m_j,2)+0.125P_a^b(m_i-m_j,2) - 0.0625P_a^b(m_i+m_j,4) - 0.0625P_a^b(m_i-m_j,4)\right). \quad (51)$$

Here, $S_r^s(p)$, $P_r^s(p,q)$ and $Q_r^s(p,q)$ are defined with following equations:

$$S_r^s(p) = \int_r^s \cos(p\pi t)dt$$

$$P_r^s(p,q) = \int_r^s \sin(pt)\sin(qt)dt$$

$$Q_r^s(p,q) = \int_r^s \cos(pt)\cos(qt)dt. \quad (52)$$

It is apparent that these three integrals have simple analytical solutions.

## ACKNOWLEDGMENT

The author would like to thank Dr. E. Mehrshahi, Iran Telecommunication Research Center, Tehran, Iran, and Dr. D. Jaggard, Electrical and Systems Engineering Department, University of Pennsylvania, Philadelphia, PA, for review of this paper's manuscript and useful comments.

## REFERENCES

[1] G. B. Hocker and W. K. Burns, "Mode dispersion in diffused channel waveguides by the effective index method," *Appl. Opt.*, vol. 16, pp. 113–118, Jan. 1977.

[2] K. Van D. Velde, H. Thienpont, and R. Van Geen, "Extending the effective index method for arbitrarily inhomogeneous optical waveguides," *J. Lightw. Technol.*, vol. 6, no. 6, pp. 1153–1159, Jun. 1988.
[3] C. M. Kim and R. V. Ramaswamy, "Modeling of graded-index channel waveguides using nonuniform finite difference method," *J. Lightw. Technol.*, vol. 7, no. 10, pp. 1581–1589, Oct. 1989.
[4] M. S. Stern, "Semivectorial polarized $H$ field solutions for dielectric waveguides with arbitrary index profiles," *Proc. Inst. Elect. Eng.*, vol. 135, pt. J, pp. 333–338, Oct. 1988.
[5] S. Akiba and H. A. Haus, "Variational analysis of optical waveguides with rectangular cross section," *Appl. Opt.*, vol. 21, pp. 804–808, Mar. 1982.
[6] B. M. A. Rahman and J. B. Davies, "Finite-element solution of integrated optical waveguides," *J. Lightw. Technol.*, vol. LT-2, no. 10, pp. 682–688, Oct. 1984.
[7] Y. Lu and F. A. Fernandez, "An efficient finite element solution of inhomogeneous anisotropic and lossy dielectric waveguides," *IEEE Trans. Microw. Theory Tech.*, vol. 41, no. 6, pp. 1215–1223, Jun./Jul. 1993.
[8] E. W. Kolk, N. H. G. Baken, and H. Blok, "Domain integral equation analysis of integrated optical channel and ridge waveguides in stratified media," *IEEE Trans. Microw. Theory Tech.*, vol. 38, no. 1, pp. 78–85, Jan. 1990.
[9] N. H. G. Baken, J. M. van Splunter, M. B. J. Diemeer, and H. Blok, "Computational modeling of diffused channel waveguides using a domain-integral equation," *J. Lightw. Technol.*, vol. 8, no. 4, pp. 576–586, Apr. 1990.
[10] H. J. M. Bastiaansen, N. H. G. Baken, and H. Blok, "Domain-integral analysis of channel waveguides in anisotropic multi-layered media," *IEEE Trans. Microw. Theory Tech.*, vol. 40, no. 10, pp. 1918–1926, Oct. 1992.
[11] H. P. Urbach and E. S. A. M. Lepelaars, "On the domain integral equation method for inhomogeneous waveguides," *IEEE Trans. Microw. Theory Tech.*, vol. 42, no. 1, pp. 118–126, Jan. 1994.
[12] P. Berini and K. Wu, "Modeling lossy anisotropic dielectric waveguides with the method of lines," *IEEE Trans. Microw. Theory Tech.*, vol. 44, no. 5, pp. 749–759, May 1996.
[13] U. Rogge and R. Pregla, "Method of lines for analysis of dielectric waveguides," *J. Lightw. Technol.*, vol. 11, no. 12, pp. 2015–2020, Dec. 1993.
[14] C. H. Henry and B. H. Verbeek, "Solution of the scalar wave equation for arbitrarily shaped dielectric waveguides by two-dimensional Fourier analysis," *J. Lightw. Technol.*, vol. 7, no. 2, pp. 308–313, Feb. 1989.
[15] D. Marcuse, "Solution of the vector wave equation for general dielectric waveguides by Galerkin method," *IEEE J. Quantum Electron.*, vol. 28, no. 2, pp. 459–465, Feb. 1992.
[16] S. J. Hewlett and F. Ladouceur, "Fourier decomposition method applied to mapped infinite domains: Scalar analysis of dielectric waveguides down to modal cutoff," *J. Lightw. Technol.*, vol. 13, no. 3, pp. 375–383, Mar. 1995.
[17] R. V. Ramaswamy and R. Srivastava, "Ion-exchange glass waveguides: A review," *J. Lightw. Technol.*, vol. 6, no. 6, pp. 984–1000, Jun. 1988.
[18] M. Koochakzadeh, R. M. Baghee, M. H. Neshati, and J. Rashed-Mohassel, "Solution of the vector wave equation for dielectric rod waveguides using the modified Fourier decomposition method," in *IRMMW-THz 2005*, Sep. 2005, vol. 2, pp. 559–560.
[19] A. Ortega-Monux, J. G. Wanguemert-Perez, L. Molina-Fernandez, E. Silvestre, and P. Andres, "Fast-Fourier based full-vectorial mode solver for arbitrarily shaped dielectric waveguides," in *MELCON*, May 2006, pp. 218–221.
[20] J. Xiao, M. Zhang, and X. Sun, "Solutions of the full- and quasi-vector wave equations based on $H$-field for optical waveguides by using mapped Galerkin method," *Opt. Commun.*, vol. 259, pp. 115–122, 2006.
[21] J. G. Wanguemert-Perez and I. Molina-Fernandez, "Analysis of dielectric waveguides by a modified Fourier decomposition method with adaptive mapping parameters," *J. Lightw. Technol.*, vol. 19, no. 10, pp. 1614–1627, Oct. 2001.
[22] J. E. Goell, "A circular-harmonic computer analysis of rectangular dielectric waveguides," *Bell Syst. Tech. J.*, pp. 2133–2160, Sep. 1969.

**Ramin Pashaie** (S'07) was born in Tehran, Iran. He received the B.S. degree in electrical engineering (with a major in microelectronics) from Shahid Beheshti University (SBU), Tehran, Iran, in 1998, the M.S. degree in fields and waves from Khaje Nasir Tousi University of Technology (KNTU), Tehran, Iran, in 2001, and is currently working toward the Ph.D. degree in electrical and system engineering at the University of Pennsylvania, Philadelphia.